15 (2022) 200092

Contents lists available at ScienceDirect

Resources, Conservation & Recycling Advances

journal homepage: www.sciencedirect.com/journal/Resources-Conservation-and-Recycling-Advances

Effect of functionalized and unfunctionalized basic oxygen steelmaking slag on the growth of cereal wheat (*Triticum aestivum*)

Lucy V. Fisher [a], Andrew R. Barron [a,b,c,d,*]

[a] Energy Safety Research Institute, Swansea University Bay Campus, Swansea, SA1 8EN, United Kingdom
[b] Arizona Institute for Resilient Environments and Societies (AIRES), University of Arizona, Tucson, Arizona 85721, United States of America
[c] Department of Chemistry and Department of Materials Science and Nanoengineering, Rice University, Houston, Texas 77005, United States of America
[d] Faculty of Engineering, Universiti Teknologi Brunei, Bandar Seri Begawan, Brunei Darussalam

ARTICLE INFO

Keywords:
Steel industry waste
Cereal wheat
Hydrophobic
Hydrophilic
Recycling
Fertilizer
Basic oxygen steelmaking slag

ABSTRACT

The continued growth of the steel industry poses concerns for the health of the planet and the health of the environment. The waste produced by the steel industry is an untapped resource that is not used nearly as much as it should be. The potential of using basic oxygen steelmaking slag (BOS) as a fertilizer was tested on cereal wheat plants' growth, with samples that are both hydrophobic and hydrophilic through functionalization. Parameters tested included: mass gain, height grown (cm), germination rate (GR), mean germination time (MGT) and a composite visual score (CVS). The results found that the BOS slag improved the growth of the samples due to the high amount of Ca and Fe provided to the sample. It was proposed that the improved performance of hydrophobically functionalized slag over those with hydrophilic functionalization was due to the water reservoir created around the seed. Lanolin functionalized samples are the optimum fertilizer in this study, providing the optimum conditions for nutrient transfer to the seed samples.

1. Introduction

Iron and steel are essential for infrastructure and allow people to live modern lives. Meaning that global steel production has reached roughly 1900 million tons annually, with this figure still expected to continue increasing (Steel Statistical Yearbook, 2020). Unfortunately, as a result, 22.6 million tons of basic oxygen steelmaking (BOS) slag waste is produced annually just in Europe (Euroslag, 2018) as a by-product of a secondary steelmaking process when pig iron is refined into steel using a basic oxygen steelmaking process. BOS slag is mainly composed of calcium silicates, iron oxides, aluminum silicates and other crystalline compounds (Fisher and Barron, 2019, 2021a; Shen and Forssberg, 2003); however, these components could be highly valuable to specific industries such as the fertilizer industry and coral reef rehabilitation industries. Such applications encourage the steelmaking industry to transition from a linear economy with high amounts of waste streams to a more circular economy where recycling is paramount.

For many years, BOS slag has been utilized in several different ways, both on land and in marine applications, including aggregate in concrete, CO_2 sequestration use, road tarmac use, pavements, railway ballast or thermal heat recovery by steelmaking slag (Reddy et al., 2006; Liu et al., 2016; Fisher and Barron, 2019, 2019; Xie et al., 2020; Sun et al., 2021; Zhao et al., 2021; Cui et al., 2021; Song et al., 2021; Yang et al., 2021). BOS slag can also create geopolymers for construction to replace traditional Portland cement in the same way fly ash has been used (Li et al., 2021; Sun et al., 2021). Electric arc furnace slag has a similar composition to BOS slag and can undergo a two-stage pyro-hydrometallurgical process in which valuable components of the slag can be recovered. The first stage is a carbothermic reduction stage in which Fe, Mn and Nb can be recovered. The second stage involves acid baking which recovers elements from the already Fe depleted slags such as Al, Ti and Mg (Kim and Azimi, 2021).

Due to BOS slag containing a high amount of $CaCO_3$, the material has become an ideal candidate for a fertilizer. Due to BOS slag's alkaline nature and other nutrients. It has previously caused crops to grow in great abundance (Branca et al., 2014). It has been previously reported that steelmaking slags can promote microalgae growth (Liu et al., 2021). Under the right conditions, the slag can promote algae reproduction and the accumulation of metabolites and encourage lipids to accumulate. The slag makes an ideal nutrient to culture the microalgae as it provides a significant source of Fe and reduces the cost of culturing microalgae. Another study assessed the leaching effect of BOS slag in agriculture

* Corresponding author.
E-mail address: a.r.barron@swansea.ac.uk (A.R. Barron).

https://doi.org/10.1016/j.rcradv.2022.200092

Available online 27 May 2022

(Branca et al., 2019). It was found that the presence of the slag increased the availability of P and Ca in the soil, and none of the heavy metals, e.g. Cr and V, that may be present in the slag leached out. In 2018 work was conducted on the ability of BOS slag to decrease CH_4 emissions and arsenic levels in rice plants (Gwon et al., 2018). In a greenhouse experiment, it was found that the grain yield of the rice plants was significantly increased by 10.3%−15.2%, and CH_4 emissions were suppressed by 17.8–24.0%. The rise in yield was attributed to the higher levels of nutrients in the soil made available by the steelmaking slag. The CH_4 reduction was attributed to the higher Fe availability, which acted as an alternate electron acceptor and decreased CH_4 emissions. Due to the formation of Fe-plaque around the roots of the plants, arsenic was sequestered (Gwon et al., 2018; Hansel et al., 2001). Research has also been conducted on the effect of power plant ash and bottom plant slag deposits on different crops such as autumn rye (*Secale cereale* L.) and barley (*Hordeum Sativum Jessen*) (Dželetović and Filipović, 1995). The characteristics of power plant ash are similar to that of BOS slag in that there are aluminosilicates and Fe, Ca and Mg. It was found that there were no adverse effects on the growth profile of the samples when grown on the deposits, and in some cases, enhanced fertilization occurred in the case of autumn rye (*Secale cereale L.*), alfalfa (*Medicago sativa* L.) and Barley (*Hordeum sativum Jessen*). The effects were not seen to be as prominent in winter rapeseed (*Brassica napus L.*) samples.

We have previously reported the effect of iron oxide particles and carbon nanotubes on wheatgrass growth, in which growth is enhanced with iron oxide particles, and the hydrophobic nature of the carbon nanotubes enhanced the growth of the seeds by providing a water reservoir for the seeds (Lee et al., 2018). In other previous work, we have reported that BOS slag has been functionalized to be both hydrophobic and hydrophilic (Fisher and Barron, 2021b). These findings led to the exploration of if the BOS slag, a known source of several plant nutrients, e.g. Ca, Fe, and Si, could be used to fertilize cereal wheat (*Triticum aestivum*) seeds and improve their growth.

2. Methods

2.1. Chemicals and materials

Basic oxygen steelmaking (BOS) slag was collected from Tata Steel, Port Talbot, South Wales, UK. We have previously reported the composition of the BOS slag used in this study (Fisher and Barron, 2021b). Rainwater was collected from Neath, South Wales, UK. Toluene, lauric acid, cysteic acid and lanolin were purchased from Sigma-Aldrich and used as received. Nitric acid and hydrochloric acid were purchased from Fisher Scientific. Isostearic acid was purchased from Tokyo Chemical Industry UK Ltd and used as received. Millipore distilled water (15 MΩ cm) was used throughout the experiments. Cereal wheat (*Triticum aestivum*) seeds were purchased from Aconbury Sprouts. Analytical reference standards for MP-AES were purchased from Sigma-Aldrich.

2.2. Functionalized BOS slag synthesis and characterization

The method used for the BOS slag synthesis was a method we have previously reported (Lee et al., 2018; Hill et al., 2019; Fisher and Barron, 2021b). In order to make the slag hydrophobic isostearic acid, lanolin and lauric acid were used. Each carboxylic acid was tested in several different ratios to find the optimum amount to functionalize the BOS slag. The appropriate carboxylic acid was refluxed overnight with 20 g of BOS slag in 200 mL of toluene. The reflux was heated and wrapped in foil at 110 °C and stirred using an overhead mechanical stirrer due to the magnetic nature of the slag. Once the reflux was completed, the solution was centrifuged at 5000 rpm for 30 min. The supernatant was then removed and disposed of, and the slag was re-dispersed in isopropanol and centrifuged. This process was repeated 3 times, and then the same process was repeated 2 times using ethanol. Once the purification was complete, the slag was dried in an oven overnight. Part of the functionalized slag was reserved for Fourier transform infrared (FTIR), and thermogravimetric analysis (TGA), and the rest was pressed into a pellet using a 32 mm dye and a pellet press. The pellet was then used for contact angle measurements. The exact process was repeated for the hydrophilic functionalized samples, which were functionalized using cysteic acid. Each reflux was also completed in triplicate.

Table 1
Summary of samples and BOS slag dosage used.

Sample number	Sample functionalization	BOS: carboxylic acid ratio	BOS Slag dosage (mg)	Qualitative visual growth rating system (Lee et al., 2018)
1	No BOS slag	N/A	0	No change
2	Unfunctionalized BOS slag	N/A	1.0	Very little to almost no root
3	Isosteric acid	1:1	1.0	Short root, no shoot
4	Isosteric acid	1:1.25	1.0	Medium length root, no shoot
5	Isosteric acid	1:1.5	1.0	Shoot (<1 cm)
6	Lauric acid	1:1	1.0	Shoot (<3 cm)
7	Lauric acid	1:1.25	1.0	Shoot (<5 cm)
8	Lauric acid	1:1.5	1.0	Shoot (<7 cm)
9	Lanolin	1:2	1.0	Shoot (<9 cm)
10	Lanolin	1:3	1.0	Shoot (<11 cm)
11	Lanolin	1:5	1.0	Shoot (<13 cm)
12	Cysteic acid	1:1	1.0	Shoot (<15 cm)
13	Cysteic acid	1:1.25	1.0	Shoot (<17 cm)
14	Cysteic acid	1:1.5	1.0	N/A

Contact angle (CA) was used to assess the degree to which the slag was functionalized, and a Krüss DSA25 Expert Drop shape machine was used for all measurements. All measurements were performed using distilled water under ambient conditions. Sessile drop water contact angle measurements were performed on the pellet in three different spots across the surface. Advanced and receding contact angle measurements were performed on three different spots on the pellet. For all measurements, the Eclipse Tangent 1 fitting method was used. TGA was performed using a TA instruments SDT Q600. The experiment was done in an open alumina crucible using continuous argon gas flow. The sample was ramped from 0 to 1000 °C at a ramp rate of 20 °C/min. From the TGA measurements grafting density was also calculated using the value of the organic weight loss. The surface area to calculate grafting density was calculated using the Brunauer-Emmett-Teller (BET) method. The surface area calculated was 31.1 ± 8.4 m^2/g. A Quantachrome Nova 2000e surface area analyzer was used for this measurement. FTIR was performed using a Thermo-fisher scientific i10 Nicolet FTIR. The scans were performed from 4000 - 400 cm^{-1}. 32 scans were performed for each sample.

2.3. Plant growth

In methods adapted from previous work, several petri dishes were filled with cotton wool (Lee et al., 2018). All of the variations of slag listed in Table 1 were tested as fertilizer. 20 seeds were grown for each variation of BOS slag in order to replicate the testing and be able to reduce error. A control sample of seeds was also grown, planted without BOS slag. The deposits of BOS slag were spaced 1 cm away from the next. Each deposit of BOS slag was weighed out using an analytical balance. The seeds were soaked in distilled water overnight before planting, as the producer of the seeds recommended. The planted seeds were placed in a dark drawer with no light. Distilled water (1 mL) was then placed on each seed for 8 days. In one instance, cereal wheat was also watered using rainwater (1 mL) to examine the effect of rainwater on cereal wheat seed growth. The pH of the water was measured using a Mettler Toledo Fivego pH meter. After the analysis was completed, the plant samples were digested using aqua regia in line with a previously

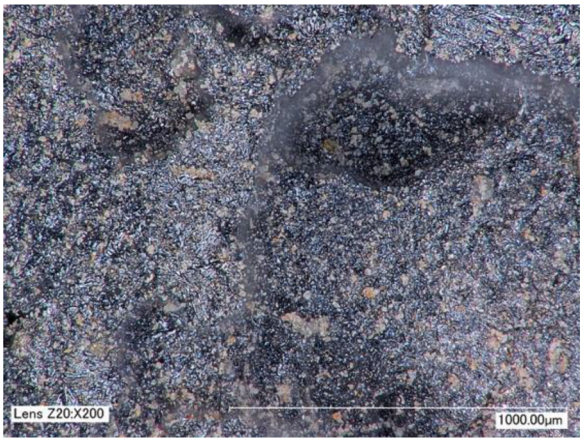

Fig. 1. Optical microscopy image of BOS slag used in the study (×200).

reported method (Rodushkin et al., 1999). The digested plant samples were then analyzed using microwave plasma atomic emission spectroscopy (MP-AES). An Agilent 4200 MP-AES was used for the analysis. Analytical reference standards were used, and the analysis was calibrated for a range of 0–20 ppm. All elements were calibrated using this range. Optical microscopy was also used to look at the plants and roots, and a Keyance VHX1000 was used for this work. The plant height data was statistically analyzed using a one-way analysis of variance (ANOVA) test with a Tukey post hoc test if required. The analysis was performed using Origin Pro 8.5 Software (Kaufmann and Schering, 2007).

3. Results and discussion

3.1. Optical microscopy

As shown from Fig. 1, the optical micrograph of the BOS slag shows a particularly rough heterogeneous texture. The image also demonstrates the material's porous nature, as a large pore can be seen in the top right-hand corner. It can be seen that dispersed within the material; several inclusions were consistent with iron oxide formed upon long-term exposure to air. Several small white particles throughout the material are consistent with $CaCO_3$ or $CaSiO_3$ since it is known that they represent a significant component of BOS slag (Fisher and Barron, 2021a; Mallick, 2018).

3.2. Plant growth

Images of the plant growth can be seen in Fig. 2, where a noticeable difference occurs between days 1, 4 and 8. On day 1, there was no change to the seeds as they had not had time to absorb the water yet and initiate the germination process, but the BOS slag deposits can be visibly seen underneath the seeds. By day 4, the seeds have germinated and sprouted roots and begun to grow a shoot, but the shoot is still very short in all cases. There is an apparent variance in the rate that the seeds germinate, as only some of the seeds can be visibly seen to have roots; this is due to the stochastic nature of the seeds. By day 8, it can be seen that all samples have grown a healthy green shoot. The shoot lengths do vary; however, the trends of variance in shoot length continued to be exhibited as there seemed to be a trend of seeds that germinated later, not being able to grow an as large shoot by day 8. For example, some of the plants in sample sets 10 and 11. The appearance of the plants is similar to that of plants seen in previous work (Lee et al., 2018).

3.3. Mass gain from plants

A plot of plant mass as a function of growth day is shown in Fig. 3. For the reference sample (i.e., no slag), the most significant rate of

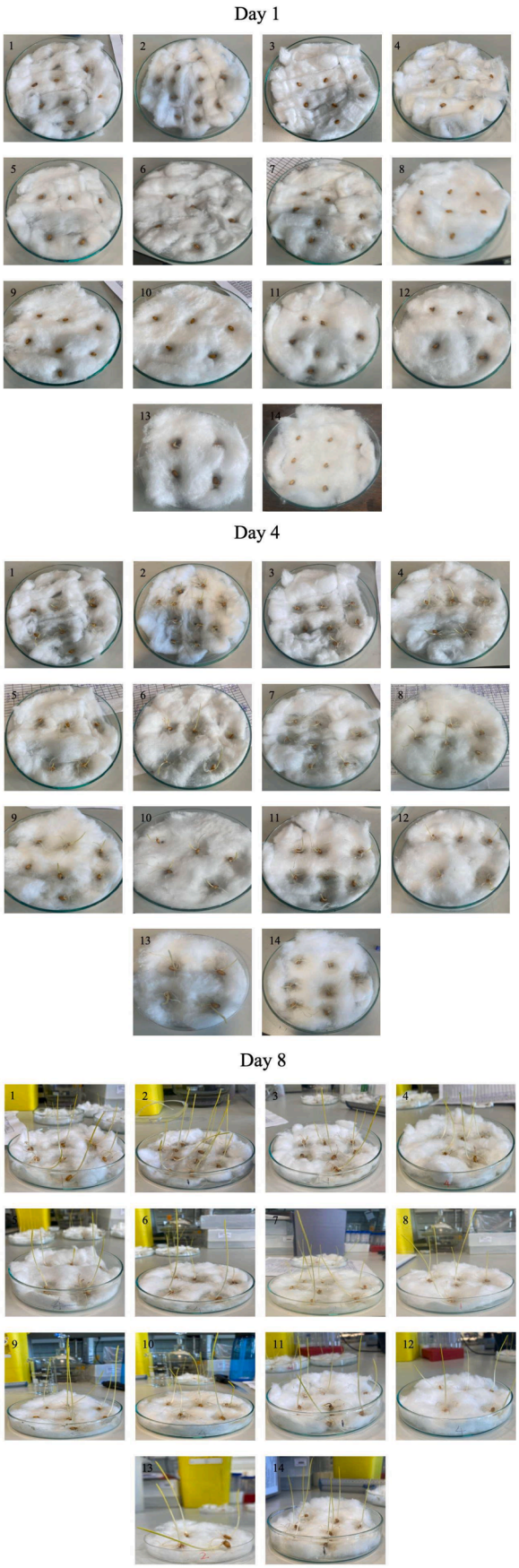

Fig. 2. Photographic images of the plant growth are shown on days 1, 4 and 8. The sample numbers correspond to those in Table 1.

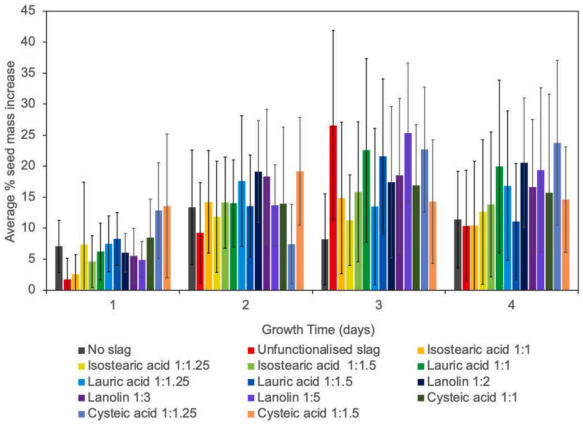

Fig. 3. Plots of seed mass gain as a function of time (days) for samples dispersed in DI water. Error bars represent one standard deviation.

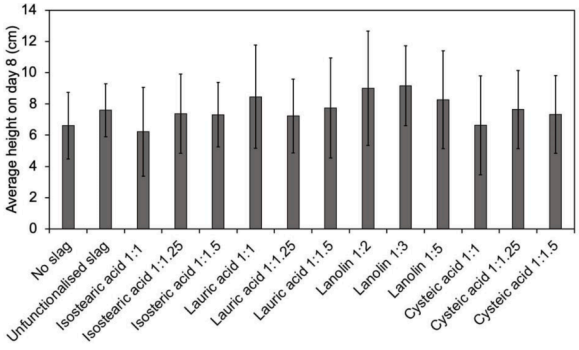

Fig. 4. Plot of average plant height after 8 days for all samples studied. Error bars represent one standard deviation.

change of mass was on day 2, whereas for the unfunctionalized BOS slag sample, the greatest change occurred on day 3. For all other samples, it can be seen that the day on which the most mass gain occurs varies between days 2 and 3 for the samples. The large standard deviation bars show much statistical variability between the seed's mass gain rates.

3.4. Average height of plants

Fig. 4 shows the average height of the seeds in each sample set on the final day (day 8). The standard deviation error bars for all the samples seem to be of similar height; the variation in plant heights has been caused by the natural variations in the plant seeds. When the sample set of plants grown with no slag and the samples grown with slag are compared, it can be seen there is a significantly better amount of growth, suggesting that the slag has worked well as fertilizer (Branca et al., 2014). The samples containing lanolin have performed the best, with a small number of the samples managing to grow over 12 cm in length (see Fig. 2 and 4). Samples containing lauric acid have managed to grow a significant amount. The similarity between lanolin and steric acid is reasonable given that lanolin is a sterol ester (even though it was traditionally called "wool fat") of various C_{12}–C_{24} carboxylic acids. Thus, lanolin, a side product from wool production, has been shown to act as a "hidden" source of long-chain carboxylic acids, c.f., lauric acid (Fisher and Barron, 2021b).

An ANOVA test was conducted across all samples to see if the slag variants significantly affected the plant growth height. The p-value used for the analysis was 0.05. The calculated p-value was 0.02, meaning the difference between the groups is statistically significant. The calculated values can be viewed below in Tables 2 and 3. A Tukey post hoc analysis test was performed in order to find out between which groups the samples were significantly different. The only samples that were significantly different from each other were Lanolin 1:3 and Isostearic acid 1:1. This comparison had a p-value of 0.05. However, none of the other samples compared were seen as being statistically different.

Table 3
ANOVA summary table of calculated values for all samples.

Source of Variation	SS	df	MS	F	P-value	F crit
Between Groups	196.70	13.00	15.13	2.02	0.02	1.76
Within Groups	1996.32	266.00	7.50			
Total	2193.02	279.00				

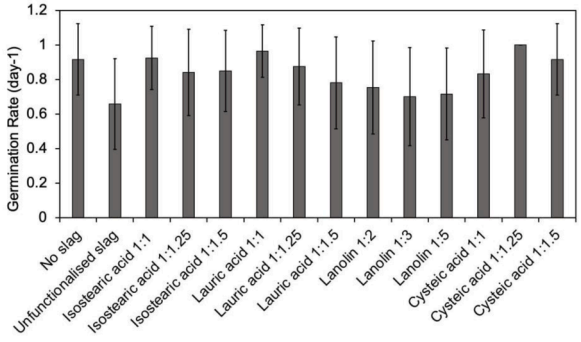

Fig. 5. Plot of mean germination rate (GR) for samples studied. Error bar represents one standard deviation.

Table 2
ANOVA variance table for all samples.

Sample number	Sample functionalization	BOS:carboxylic acid ratio	Count	Sum	Average	Variance
1	No BOS slag	N/A	20	132.20	6.61	4.52
2	Unfunctionalized BOS slag	N/A	20	151.40	7.57	2.79
3	Isostearic acid	1:1	20	124.40	6.22	8.07
4	Isostearic acid	1:1.25	20	147.50	7.38	6.41
5	Isosteric acid	1:1.5	20	146.30	7.32	4.27
6	Lauric acid	1:1	20	169.30	8.47	10.92
7	Lauric acid	1:1.25	20	144.60	7.23	5.59
8	Lauric acid	1:1.5	20	155.00	7.75	10.27
9	Lanolin	1:2	20	180.30	9.02	13.40
10	Lanolin	1:3	20	183.30	9.17	6.51
11	Lanolin	1:5	20	165.50	8.28	9.85
12	Cysteic acid	1:1	20	132.70	6.64	10.00
13	Cysteic acid	1:1.25	20	152.80	7.64	6.24
14	Cysteic acid	1:1.5	20	146.60	7.33	6.24

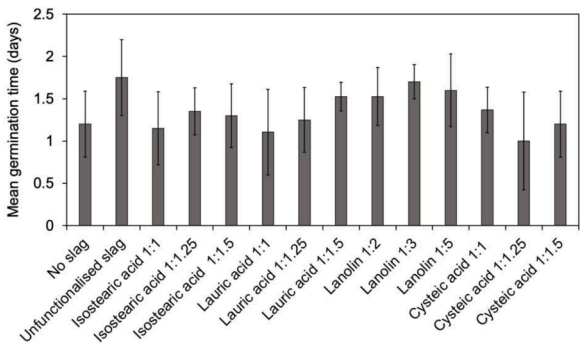

Fig. 6. Plot of mean germination time (MGT) for samples studied. Error bar represents one standard deviation.

3.5. Germination rate

The germination rate (GR) was observed to be similar for all the slag samples (Fig. 5), although the GR for the sample grown with no slag (0.92 day^{-1}) is faster than that for the unfunctionalized BOS slag (0.66 day^{-1}). This suggests that the presence of BOS slag inhibits germination. Nevertheless, the functionalized slag samples perform better than unfunctionalized. While the standard deviation bars are large, the hydrophobic functionalized slag samples (isosteric, lauric and lanolin) show a decreasing germination rate with increasing functionality (and hence hydrophobicity). The MGT in Fig. 6 is in line with the GR as it shows that samples with a slower rate of germination took longer to germinate.

3.6. Composite visual score graphs (CVS)

The CVS graphs in Fig. 7 show that all the samples seem to grow at a similar rate, as all the graphs seem to follow a similar S-like curve pattern. On days 3–6 for most samples, the error bars from standard deviation on most of the samples are small, showing that there is little to no variance in the growth of the plants in the middle of the growing stage. However, past day 6, it can be seen that large error bars are saying that there is variance in how well the plants perform beyond this point. This is again due to the variance between the different cereal wheat seeds. If the no slag sample and unfunctionalized sample are compared, it can be seen that they follow a similar rate of growth.

3.7. Microwave plasma atomic emission spectroscopy (MP-AES)

Although BOS slag is predominantly calcium silicates, iron oxides, and aluminum silicates, it contains a wide range of trace elements (Fisher and Barron, 2021a), some of which may be undesirable to be up-taken into plants. In order to determine the effects of the slag on the plants, MP-AES was employed, and the results are shown in Table 4.

Notably, there appears to be no statistical change in the presence of Al, Mg, Mn, and Zn between samples with slag and the reference without slag. In contrast, P shows a slight decrease in uptake for all the slag samples compared to the reference, while Si is slightly increased; however, the ubiquitous nature of silicon makes analysis difficult (Doostdar et al., 2011). There is a marked increase in Cu for the sample grown on raw slag but no effect on the functionalized slag samples. We propose that the carboxylic acid covalent functionality on the surface (Bethley et al., 1997; Koide and Barron, 1995) inhibits its leaching out of the slag. Interestingly, Fe is seen to leach out of the unfunctionalized slag but not the hydrophobic versions. Finally, an increase in Ca is found in all the plants grown on the unfunctionalized and hydrophobic slags compared to the reference sample and plants grown with hydrophilic functionalized slag (i.e., cysteic acid functionalized).

Fig. 8 shows an optical microscopy image of a plant root from the unfunctionalized sample set that has been watered with DI water. It can be seen that in the root, there is a black particle, which could be particles of the slag entrained.

3.8. Functionality versus growth

From the data, it can be said that the BOS slag had a positive effect on the growth of the cereal wheat seeds. This is because of the high amount of Ca present in the BOS slag samples, an essential mineral for plant growth, which assists with cell structure, elongation, and division (Hepler, 2005). Between the unfunctionalized and functionalized slags, it was found that the best fertilizer for the plants was BOS slag functionalized with lanolin in a 1:3 ratio. This sample set was seen to have the highest average height overall, with 9.17 cm. The highest mass gain for this seed was seen on day 2, with the GR rate being slower also. This sample also has a higher amount of Fe (Table 4), a slight increase in Al, retention of Mg, but no increase of undesirable elements. Al has been previously reported to increase root growth in low concentrations (Uchida, 2000). In previous studies, Fe has been shown to encourage plant enzyme production and speed up the metabolism of the plants (Rout and Sahoo, 2015). Mg also contributes to enzyme activity in plants (Shaul, 2002).

The increased mass gain of the sample on day 2 may be due to the high Ca content recorded by the MP-AES measurements at 0.68 ppm. This suggests that the high Ca content encourages faster cell structure formation and cell elongation leading to the mass gain on day 2. It can be said that the lanolin component of the sample also played a role in the increased plant growth. Lanolin is a natural lubricant and has been used in plant research as a carrier for plant growth regulators (Wu et al., 2020; Lv et al., 2021; Redemann et al., 1950). The lanolin does not have a physiological effect on the plant tissue but instead allows the easier transport of nutrients towards the seed.

3.9. Distilled water versus rainwater

Fig. 9 shows images comparing the plants grown with no BOS slag, with unfunctionalized BOS slag watered with distilled water (DI water) and unfunctionalized BOS slag watered with rainwater. It can be seen that there is no noticeable difference between the seeds on day 1 as the seeds have not yet had enough time to absorb water and germinate. On day 4, all sample sets have evidence of considerable root growth, with some shoots being present. On day 8, it can be seen that all the samples set have grown a considerable shoot with there being some variation in the height of the plants.

Fig. 10 shows the mass gain of the 3 sample sets over a 4-day period, where it can be seen that there is the most significant mass gain by the rainwater sample set on day 3. This follows a similar pattern to the other samples fertilized with BOS slag. The sample grown without any BOS slag being present had the best growth rate on day 2. However, the average height data in Fig. 11 shows that the sample set watered with DI water performed better during the height measurements than the sample watered with rainwater. It can also be seen that the sample set grown with no BOS slag performed better in the height measurements.

Nevertheless, it can be seen from the variance in the standard deviation error bars on the graph that, in some cases, the samples did grow to be taller than the sample set with no BOS slag. The samples were again subjected to ANOVA analysis with a p-value of 0.05. The calculated p-value for the variance between samples was 0.083, suggesting no significant statistical difference between the samples and, therefore, no difference between the samples grown with rainwater vs DI water. The ANOVA summary data can be seen in Tables 5 and 6.

Samples watered with rainwater have germinated faster than those watered with DI water but not as fast as the sample set grown with no BOS slag, as shown in Fig. 12. The GR of the DI water unfunctionalized sample was 0.66 day^{-1}, and the rainwater sample was 0.79 day^{-1}. So, with the addition of rainwater watering, it can be said that the addition

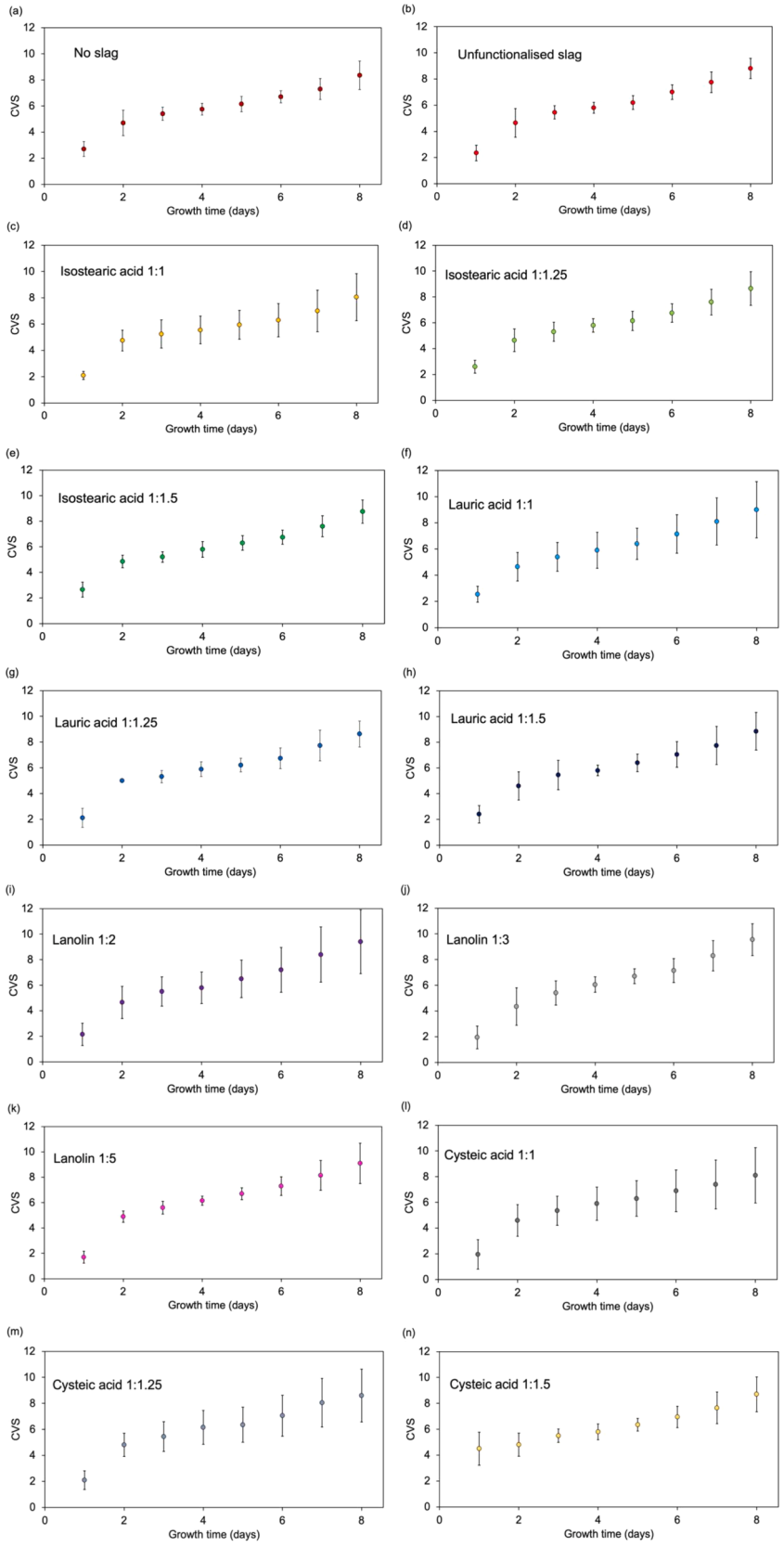

Fig. 7. Plots (a-n) of composite visual growth scores (CVS) for samples studied. Error bars represent one standard deviation.

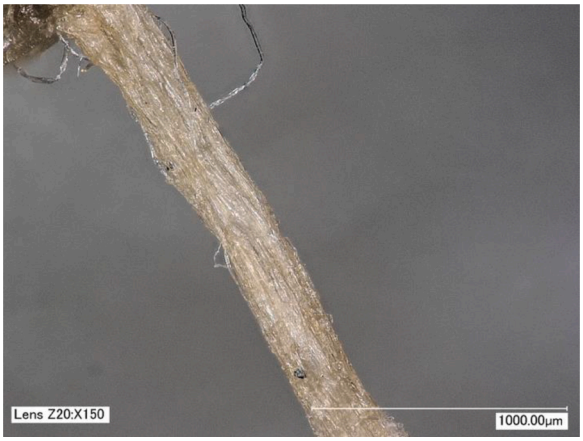

Fig. 8. Optical microscopy image of sample 2 plant root (×200).

of rainwater increases the GR rate. The MGT graph in Fig. 13 shows that rainwater samples germinated faster than the sample watered with DI water.

The CVS graph depicting the growth of the sample watered with rainwater is shown in Fig. 14 and can be seen to follow an S like pattern where the rate of change is rapid towards the start, slower towards the middle. Then the change begins to happen faster again towards day 8. Nevertheless, there is a significant variance between the different samples in the sample set, as seen in the standard deviation error bars on the graph.

In the MP-AES data shown in Table 7, it may be seen that the elemental uptake is generally directly proportional to the composition of the water source. The exception is that the high Ca content in rainwater is not replicated by the uptake for the sample with unfunctionalized slag, suggesting that the Ca is absorbed onto the slag rather than the plant. In contrast, there is also a direct correlation with DI water, except that Cu is leached from the slag into the plants.

We note that the calcium content of the rainwater was measured as having a value of 12.35 ppm, not in line with previous data recorded for rainwater from the South Wales area. Previous recordings of Rainwater in South Wales have had readings ranging between 0.085–0.448 ppm (DEFRA 2021). This suggests that when the rainwater fell, the precipitation had been transported from an area with high calcium levels in the rainwater.

It was found that the rainwater had a pH reading of 6.89, and the DI water had a pH reading of 7.03. When the data is compared of samples watered with rainwater and samples watered with DI water, it is clear that the DI water was better for plant growth as these plants grew taller and germinated faster than the other plants. This suggests that high levels of Ca can inhibit plant growth. This has previously been reported that growth is inhibited when cereal wheat is grown with Ca in a 500 µg/mL concentration (He et al., 2018). This is due to calcium toxicity, which has previously been reported when excess calcium is detected within the rhizosphere, the area around the roots, then plant growth rates and germination rates are inhibited (White and Broadley, 2003).

4. Conclusions

Overall it can be concluded that the BOS slag worked well as a fertilizer for the samples. This can be seen from the fact that after day 8, a large proportion of the sample sets grew taller than the control set grown with no BOS slag. This can be due to the Ca and Fe nutrients that the BOS slag has provided to the cereal wheat seed. It could be seen that samples functionalized with carboxylic acids to become hydrophobic worked the best because of the water reservoir created around the rhizosphere by the hydrophobic slag; this is in line with previous reports (Lee et al., 2018). The data also shows that the sample functionalized with cysteic acid did not work as well as fertilizer due to the hydrophilic water-loving nature of the sample, where the water may have been absorbed too quickly by the slag before the seed sample had enough time to absorb the water. We propose that the use of lanolin makes a viable reagent as a low cost sustainable hydrophobic functionalization for BOS slag. It must be noted that the ANOVA tests showed that none of the results were statistically significant. This may suggest that there is no relationship between the BOS slag as fertilizer or that the sample size for the experiment

Table 4
MP-AES data for all samples. The error represents one standard deviation.

Sample number	Sample	Al(ppm)	Ca(ppm)	Cu(ppm)	Fe(ppm)	K(ppm)	Mg(ppm)	Mn(ppm)	P(ppm)	Si(ppm)	Zn(ppm)
1	No BOS slag	0.03 ± 0.01	0.18 ± 0.04	0.02 ±0.01	0.12 ± 0.12	1.48 ± 0.06	0.52 ± 0.11	0.04 ± 0.01	1.47 ± 0.19	0.05 ± 0.02	0.02 ± 0.01
2	Unfunctionalized BOS slag	0.04 ± 0.02	0.35 ± 0.05	0.52 ± 0.22	0.21 ± 0.10	1.34 ± 0.06	0.45 ± 0.06	0.03 ± 0.01	1.29 ± 0.09	0.10 ± 0.03	0.05 ± 0.02
3	Isostearic acid 1:1	0.06 ± 0.01	0.27 ± 0.04	0.08 ± 0.06	0.01 ± 0.01	1.28 ± 0.16	0.45 ± 0.07	0.02 ± 0.01	1.29 ± 0.24	0.08 ± 0.01	0.02 ± 0.01
4	Isostearic acid 1:1.25	0.18 ±0.16	0.53 ± 0.32	0.07 ± 0.03	0.36 ± 0.01	2.80 ± 2.22	0.45 ± 0.04	0.04 ± 0.02	1.12 ± 0.05	0.28 ± 0.24	0.03 ± 0.03
5	Isostearic acid 1:1.5	0.11 ± 0.1	0.39 ± 0.11	0.08 ± 0.04	0.14 ± 0.01	1.35 ± 0.08	0.47 ± 0.01	0.02 ± 0	1.30 ± 0.05	0.14 ± 0.08	0.02 ± 0.01
6	Lauric acid 1:1	0.03 ± 0.01	0.28 ± 0.06	0.08 ± 0.09	0.14 ± 0.07	1.25 ± 0.09	0.40 ± 0.02	0.02 ± 0.01	1.15 ± 0.07	0.07 ± 0.01	0.05 ± 0.05
7	Lauric acid 1:1.25	0.08 ± 0.08	0.37 ± 0.22	0.02 ± 0.01	0.31 ± 0.33	1.38 ± 0.14	0.41 ± 0.09	0.06 ± 0.05	1.14 ± 0.05	0.09 ± 0.07	0.03 ± 0.02
8	Lauric acid 1:1.5	0.09 ± 0.01	0.52 ± 0.29	0.05 ± 0.03	0.34 ± 0.32	1.58 ± 0.49	0.53 ± 0.12	0.05 ± 0.03	1.38 ± 0.05	0.13 ± 0.07	0.04 ± 0.02
9	Lanolin 1:2	0.03 ± 0.01	0.30 ± 0.02	0.02 ± 0.01	0.11 ± 0.03	1.13 ± 0.04	0.36 ± 0.05	0.02 ± 0.01	0.99 ± 0.08	0.08 ± 0.03	0.02 ± 0
10	Lanolin 1:3	0.08 ± 0.07	0.68 ± 0.56	0.01 ± 0.01	0.37 ± 0.37	1.22 ± 0.18	0.60 ± 0.19	0.06 ± 0.05	1.30 ± 0.09	0.14 ± 0.10	0.03 ± 0.01
11	Lanolin 1:5	0.05 ± 0.02	0.38 ± 0.04	0.01 ± 0.01	0.15 ± 0.04	1.48 ± 0.01	0.55 ± 0.01	0.04 ± 0.02	1.37 ± 0.06	0.10 ± 0.01	0.02 ± 0.01
12	Cysteic acid 1:1	0.01 ± 0	0.18 ± 0.02	0.01 ± 0.01	0.02 ± 0.01	1.02 ± 0.13	0.32 ± 0.03	0.01 ± 0	0.84 ± 0.10	0.03 ± 0.01	0.00 ± 0.01
13	Cysteic acid 1:1.25	0.02 ± 0.01	0.17 ± 0.05	0.01 ± 0.01	0.05 ± 0.02	1.50 ± 0.27	0.45 ± 0.02	0.01 ± 0.01	1.30 ± 0.19	0.03 ± 0.01	0.02 ± 0.01
14	Cysteic acid 1:1.5	0.01 ± 0.01	0.14 ±0.02	0.01 ± 0.01	0.02 ± 0.01	1.61 ± 0.05	0.51 ± 0.01	0.01 ± 0	1.45 ± 0.07	0.03 ± 0.01	0.01 ± 0.01

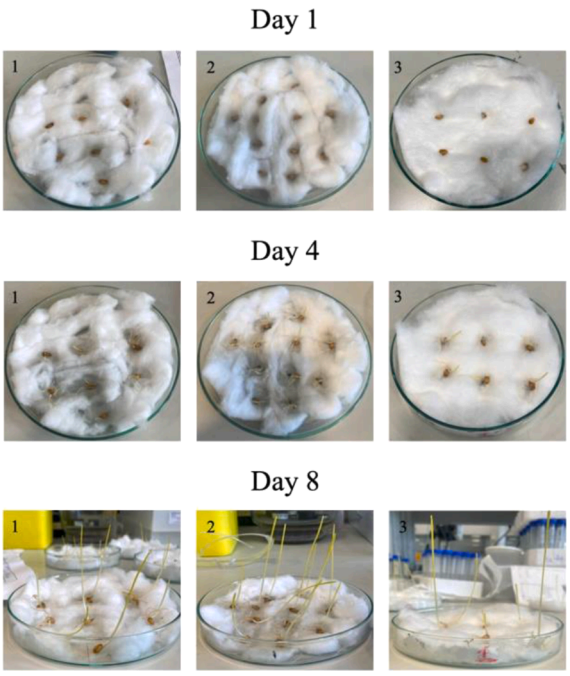

Fig. 9. Photographic images of the plant growth shown on days 1, 4 and 8 for Sample 1 (no slag), sample 2 (unfunctionalized slag with DI water), and sample 3 (unfunctionalized slag with rainwater).

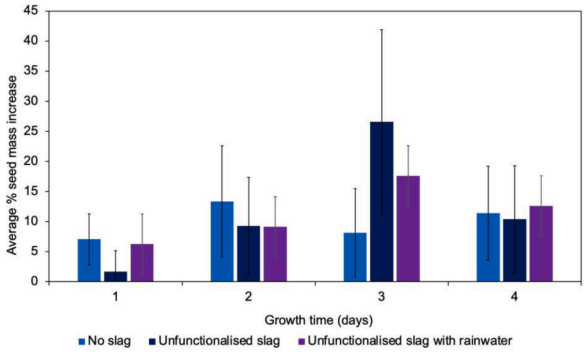

Fig. 10. Plots of seed mass gain as a function of time (days). Error bars represent one standard deviation.

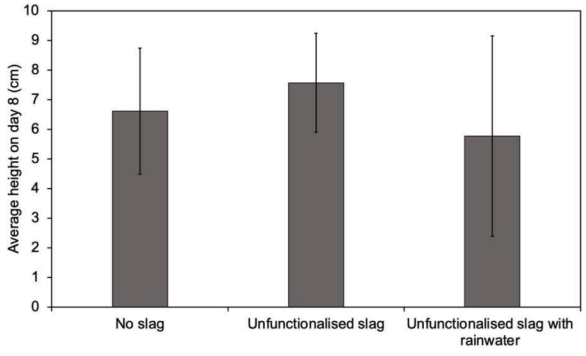

Fig. 11. Plot of average plant height after 8 days for all samples studied. Error bars represent one standard deviation.

was not large enough to gather enough data on the effects of the BOS slag on the cereal wheat seed.

If BOS slag is to be used as fertilizer, it should be noted that the concentration of heavy metals, e.g. V and Cr, in the BOS slag should be screened to check that the concentration is not over the limit and will not do harm to the environment around it. In this case, DI water produced the best results instead of rainwater due to the high Ca content of the rainwater, which may have caused calcium toxicity to occur in the seed, meaning that the growth of the sample was potentially stunted. This research can be useful in arid regions where water is scarce and is absorbed too quickly by the soil for the seed to get the full benefit, as a hydrophobic layer of slag can be used to create a water reservoir that would provide both water and nutrients to the seed.

Table 5
ANOVA variance table for No slag, Unfunctionalized slag and Unfunctionalized slag with rainwater.

Groups	Count	Sum	Average	Variance
No slag	20.00	132.20	6.61	4.52
Unfunctionalized slag	20.00	151.40	7.57	2.79
Rainwater	20.00	115.40	5.77	11.44

Table 6
ANOVA summary table of calculated values for No slag, Unfunctionalized slag and Unfunctionalized slag with rainwater.

Source of Variation	SS	df	MS	F	P-value	F crit
Between Groups	32.45	2.00	16.22	2.60	0.08	3.16
Within Groups	356.32	57.00	6.25			
Total	388.77	59.00				

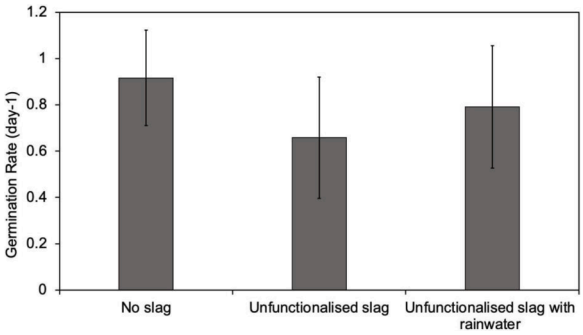

Fig. 12. Plot of mean germination rate (GR) for samples studied. Error bar represents one standard deviation.

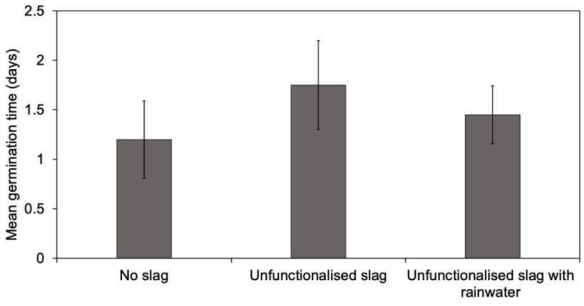

Fig. 13. Plot of mean germination time (MGT) for samples studied. Error bar represents one standard deviation.

Declaration of Competing Interest

The authors declare that they have no known competing financial interests or personal relationships that could have appeared to influence

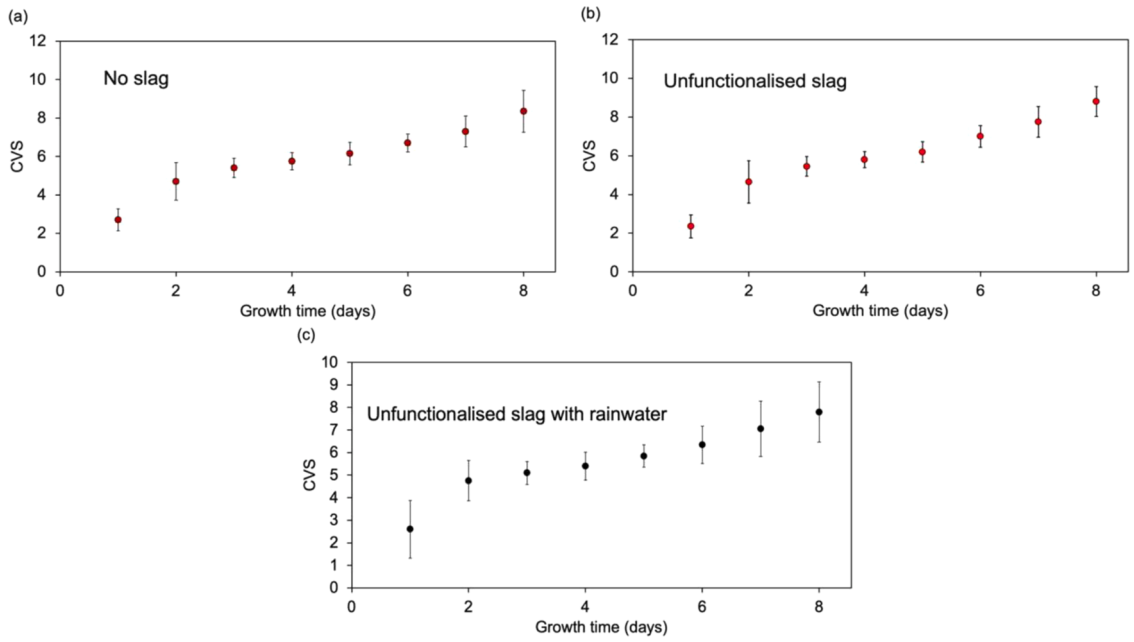

Fig. 14. Plots of composite visual growth scores (CVS) for samples studied for (a) no slag, (b) unfunctionalized slag with DI water, and (c) unfunctionalized slag with rainwater. Error bars represent one standard deviation.

Table 7
MP-AES data for all samples. The error represents one standard deviation.

Sample	Al(ppm)	Ca(ppm)	Cu(ppm)	Fe(ppm)	K(ppm)	Mg(ppm)	Mn(ppm)	P(ppm)	Si(ppm)	Zn(ppm)
No BOS slag with DI water	0.03 ± 0.01	0.18 ± 0.04	0.02 ±0.01	0.12 ± 0.12	1.48 ± 0.06	0.52 ± 0.11	0.04 ± 0.01	1.47 ± 0.19	0.05 ± 0.02	0.02 ± 0.01
Unfunctionalized BOS slag with DI water	0.04 ± 0.02	0.35 ± 0.05	0.52 ± 0.22	0.21 ± 0.10	1.34 ± 0.06	0.45 ± 0.06	0.03 ± 0.01	1.29 ± 0.09	0.10 ± 0.03	0.05 ± 0.02
Unfunctionalized BOS slag with rainwater	0.02 ± 0	0.22 ± 0.14	0.01 ± 0.01	0.11 ± 0.02	1.80 ± 0.27	0.52 ± 0.08	0.02 ± 0.01	1.31 ± 0.21	0.07 ± 0.03	0.02 ± 0.01
DI water	0.01	0.16	0.01	0.1	1.22	0.68	0.02	1.45	0.51	0.01
Rainwater	0.02	12.35	0.01	0.11	1.81	0.60	0.02	1.31	0.5	0.01

the work reported in this paper.

Acknowledgments

The AIM facility provided access to the Keyance VHX1000, and we would like to acknowledge the assistance provided by Swansea University College of Engineering AIM Facility, which was funded in part by the EPSRC (EP/M028267/1), and the European Regional Development Fund through the Welsh Government (80708). Additional support is provided by the Reducing Industrial Carbon Emissions (RICE) operations funded by the Welsh European Funding Office (WEFO) through the Welsh Government.

References

Bethley, C.E., Aitken, C.L., Koide, Y., Harlan, C.J., Bott, S.G., Barron, A.R., 1997. Structural characterization of dialkylaluminum carboxylates: models for carboxylate alumoxanes. Organometallics 16, 329–341. https://doi.org/10.1021/om960576q.

Branca, T.A., Fornai, B., Colla, V., Pistocchi, C., Ragaglini, G., 2019. Application of basic oxygen furnace (BOFs) in agriculture: a study on the economic viability and effects on the soil. Environ. Eng. Manag. J. 18, 1231–1244. https://doi.org/10.30638/eemj.2019.118.

Branca, T.A., Pistocchi, C., Colla, V., Ragaglini, G., Amato, A., Tozzini, C., Mudersbach, D., Morillon, A., Rex, M., Romaniello, L., 2014. Investigation of (BOF) Converter slag use for agriculture in Europe. Metall. Res. Technol. 111, 155–167. https://doi.org/10.1051/metal/2014022.

Cui, P., Wu, S., Xiao, Y., Liu, Q., Wang, F., 2021. Hazardous characteristics and variation in internal structure by hydrodynamic damage of BOF slag-based thin asphalt overlay. J. Hazard. Mater. 412, 125344 https://doi.org/10.1016/j.jhazmat.2021.125344.

DEFRA. DEFRA UKEAP: precip-net rainwater data for Ystradffin [Internet]. 2021 [cited 2021 Dec 8]. Available from: https://uk-air.defra.gov.uk/data/non-auto-data?uka_id=UKA00505amp;view=data&network=ukeap&year=2021&pollutant=747#view.

Doostdar, N., Smith, C., Hamill, M.B., Barron, A.R., 2011. Synthesis of calcium-silica composites: a route towards an in-vitro model system for calcific band keratopathy precipitates. J. Biomed Mater. Res. 173–183. https://doi.org/10.1002/jbm.a.33172, 99ADOI.

Dželetović, Ž., Filipović, R., 1995. Grain characteristics of crops grown on power plant ash and bottom slag deposit. Resour. Conserv. Recycl. 13, 105–113. https://doi.org/10.1016/0921-3449(94)00040-C.

Euroslag. Euroslag 2018 Statistics [Internet]. 2018 [cited 2021 Dec 8]. Available from: https://www.euroslag.com/products/statistics/statistics-2018/.

Fisher, L.V., Barron, A.R., 2019. The recycling and reuse of steelmaking slags - A review. Resour. Conserv. Recycl. 146, 244–255. https://doi.org/10.1016/j.resconrec.2019.03.010.

Fisher, L.V., Barron, A.R., 2021a. Suitability of steel making slag as a construction material resource. Recent Progress in Mater. 3, 17. https://doi.org/10.21926/rpm.2103028.

Fisher L.V., Barron, A.R., 2021b. Functionalization of basic oxygen steelmaking slag. AIP Conf. Proc., in press.

Gwon, H.S., Khan, M.I., Alam, M.A., Das, S., Kim, P.J., 2018. Environmental risk assessment of steelmaking slags and the potential use of LD slag in mitigating methane emissions and the grain arsenic level in rice (Oryza sativa L.). J. Hazard. Mater. 353, 236–243. https://doi.org/10.1016/j.jhazmat.2018.04.023.

Hansel, C.M., Fendorf, S., Sutton, S., Newville, M., 2001. Characterization of Fe plaque and associated metals on the roots of mine-waste impacted aquatic plants. Environ. Sci. Technol. 35, 3863–3868. https://doi.org/10.1021/es0105459.

He, J., Li, R., Sun, X., Wang, W., Hu, J., Xie, H., Yin, H., 2018. Effects of calcium alginate submicroparticles on seed germination and seedling growth of wheat (triticum aestivum L.). Polymers (Basel) 10, 1154. https://doi.org/10.3390/polym10101154.

Hepler, P., 2005. Calcium: a central regulator of plant growth and development. Plant Cell 17, 2142–2155. https://doi.org/10.1105/tpc.105.032508.

Hill, D., Barron, A.R., Alexander, S., 2019. Comparison of hydrophobicity and durability of functionalized aluminium oxide nanoparticle coatings with magnetite

nanoparticles–links between morphology and wettability. J. Colloid Interface Sci. 555, 323–330. https://doi.org/10.1016/j.jcis.2019.07.080.
Kaufmann, J., Schering, A., 2007. Analysis of Variance ANOVA. Wiley Encyclopedia of Clin. Trials. https://doi.org/10.1002/9780471462422.eoct017.
Kim, J., Azimi, G., 2021. Valorization of electric arc furnace slag via carbothermic reduction followed by acid baking – water leaching. Resour. Conserv. Recycl. 173, 105710 https://doi.org/10.1016/j.resconrec.2021.105710.
Koide, Y., Barron, A.R., 1995. [Al5(tBu)5(μ3-O)2(μ3-OH)3(μ-OH)2(μ-O2CPh)2]: a model for the interaction of carboxylic acids with boehmite. Organometallics 14, 4026–4029. https://doi.org/10.1021/om00008a060.
Lee, S.M., Raja, P.M.V., Esquenazi, G.L., Barron, A.R., 2018. Effect of raw and purified carbon nanotubes and iron oxide nanoparticles on the growth of wheatgrass prepared from the cotyledons of common wheat (triticum aestivum). Environ. Sci.: Nano. 5, 103–114. https://doi.org/10.1039/C7EN00680B.
Li, Z., Fei, M., Huyan, C., Shi, X., 2021. Nano-engineered, fly ash-based geopolymer composites: an overview. Resour. Conserv. Recycl. 168, 105334 https://doi.org/10.1016/j.resconrec.2020.105334.
Liu, C., Guo, M., Pandelaers, L., Blanpain, B., Huang, S., 2016. Stabilization of free lime in BOF slag by melting and solidification in air. Metall. Mater. Trans. B 47, 3237–3240. https://doi.org/10.1007/s11663-016-0809-4.
Liu, H., Zhu, B., Wei, H., Chai, C., Chen, Y., 2019. Laboratory evaluation on the performance of porous asphalt mixture with steel slag for seasonal frozen regions. Sustainability 11, 6924. https://doi.org/10.3390/su11246924.
Liu, T., Wang, Y., Zeng, Y., Li, J., Yu, Q., Wang, X., Gao, D., Wang, F., Cai, S., Zeng, Y., 2021. Effects from Fe, P, Ca, Mg, Zn and Cu in steel slag on growth and metabolite accumulation of microalgae: a review. Appl. Sci. 11, 6589. https://doi.org/10.3390/app11146589.
Lv, J., Chen, Y.-.Q., Ding, A.-.M., Lei, B., Yu, J., Gao, X.-.M., Sai, C.-.B., Sun, .Y..-H., 2021. Control of axillary bud growth in tobacco through toxin gene expression system. Sci. Rep. 11, 17513. https://doi.org/10.1038/s41598-021-96976-3.
Mallick, P.K., 2018. 2.18 Particulate Filled and Short Fiber Reinforced Polymer Composite in Comprehensive Composite Materials II. Ed. Beaumont, P.W.R., Zweben, C.H., Elsevier, 360–400. 10.1016/B978-0-12-803581-8.03837-6.
Reddy, A.S., Pradhan, R.K., Chandra, S, 2006. Utilization of basic oxygen furnace (BOF) slag in the production of a hydraulic cement binder. Int. J. Miner. Process. 79, 98–105. https://doi.org/10.1016/j.minpro.2006.01.001.
Redemann, C.T., Wittwer, S.H., Sell, H.M., 1950. Precautions in the use of lanolin as an assay diluent for plant growth substances. Plant Physiol. 25, 356–358. https://doi.org/10.1104/pp.25.2.356.
Rodushkin, I., Ruth, T., Huhtasaari, A., 1999. Comparison of two digestion methods for elemental determinations in plant material by ICP techniques. Anal. Chim. Acta. 378, 191–200. https://doi.org/10.1016/S0003-2670(98)00635-7.
Rout, G., Sahoo, S., 2015. Role of iron in plant growth and metabolism. Rev. Agric. Sci. 3, 1–24. https://doi.org/10.7831/ras.3.1.
Shaul, O., 2002. Magnesium transport and function in plants: the tip of the iceberg. BioMetals 15, 307–321. https://doi.org/10.1023/a:1016091118585.
Shen, H., Forssberg, E., 2003. An overview of recovery of metals from slags. Waste Manag. 23, 933–949. https://doi.org/10.1016/S0956-053X(02)00164-2.
Song, Q., Guo, M., Wang, L., Ling, T., 2021. Use of steel slag as sustainable construction materials: a review of accelerated carbonation treatment. Resour. Conserv. Recycl. 173, 105740 https://doi.org/10.1016/j.resconrec.2021.105740.
Steel Statistical Yearbook 2020. Worldsteel committee on economic studies, (Brussels, 2020). https://www.worldsteel.org/en/dam/jcr:5001dac8-0083-46f3-aadd-35aa357acbcc/Steel%2520Statistical%2520Yearbook%25202020%2520%2528concise%2520version%2529.pdf. Cited December 11, 2021.
Sun, K., Peng, X., Chu, S.H., Wang, S., Zeng, L., Ji, G., 2021. Utilization of BOF steel slag aggregate in metakaolin-based geopolymer. Constr. Build. Mater. 300, 124024 https://doi.org/10.1016/j.conbuildmat.2021.124024.
Uchida, R., 2000. Essential nutrients for plant growth: nutrient functions and deficiency symptoms. In plant nutrient management in hawaii's soils, approaches for tropical and subtropical agriculture. Ed. Silva, J.A., University of Hawaii at Manoa, College of Agriculture & Tropical Resources, p. 31–55. ISBN-10:1929325088.
White, P.J., Broadley, M.R., 2003. Calcium in plants. Ann. Bot. 92, 487–511. https://doi.org/10.1093/aob/mcg164.
Xie, J., Yang, C., Zhang, L., Zhou, X., Wu, S., Ye, Q., 2020. Investigation of the physic-chemical properties and toxic potential of basic oxygen furnace slag (BOF) in asphalt pavement constructed after 15 years. Constr. Build. Mater. 238, 117630 https://doi.org/10.1016/j.conbuildmat.2019.117630.
Wu, T., Liu, H.-.T., Zhao, G.-.P., Song, J.-.X., Wang, X.-.L., Yang, C.-.Q., Zhai, R., Wang, Z.-.G., Ma, F.-.W., Xu, L.-.F., 2020. Jasmonate and ethylene-regulated ethylene response factor 22 promotes lanolin-induced anthocyanin biosynthesis in 'zaosu' pear (pyrus bretschneideri rehd.) fruit. Biomolecules 10, 278. https://doi.org/10.3390/biom10020278.
Yang, J., Firsbach, F., Sohn, I., 2021. Pyrometallurgical processing of ferrous slag "co-product" zero waste full utilization: a critical review. Resour. Conserv. Recycl. 178, 106021 https://doi.org/10.1016/j.resconrec.2021.106021.
Zhao, Y., Sun, P., Chen, P., Guan, X., Wang, Y., Liu, R., Wei, J., 2021. Component modification of basic oxygen furnace slag with C4AF as target mineral and application. Sustainability 13, 6536. https://doi.org/10.3390/su13126536.